

Integrated Transformer with Buried Windings in Ferrite Core

**Mahamat Ahmat Taha^{1,2,*}, Mahamat Hassan Bechir^{1,2}, Ouzer Nabil Adam^{1,2},
Arafat Ousman Bechir^{1,2}, Boukhari Mahamat Issa^{1,2}, Yaya Dagal Dari^{1,2}, David Pietroy¹,
Jean Jacques Rousseau¹**

¹Hubert Curien Laboratory, Jean Monnet University of Saint Etienne, Saint Etienne, France

²Department of Electrical Engineering, National Institute of Science and Technology of Abeche, Abeche, Chad

Email address:

mahamat.taha@yahoo.fr (M. A. Taha), mahassan1025@yahoo.fr (M. H. Bechir), arafat.ousman@yahoo.fr (A. O. Bechir)

*Corresponding author

To cite this article:

Mahamat Ahmat Taha, Mahamat Hassan Bechir, Ouzer Nabil Adam, Arafat Ousman Bechir, Boukhari Mahamat Issa, Yaya Dagal Dari, David Pietroy, Jean Jacques Rousseau. Integrated Transformer with Buried Windings in Ferrite Core. *Journal of Electrical and Electronic Engineering*. Vol. 10, No. 1, 2022, pp. 10-17. doi: 10.11648/j.jee.20221001.12

Received: January 15, 2022; **Accepted:** January 27, 2022; **Published:** February 9, 2022

Abstract: In the field of electronics, one of the objectives of current research is to integrate numerous components in increasingly smaller volumes. Reducing the cost of manufacturing components requires integration and collective manufacturing. This paper mainly focuses on the design and the main steps of the micro-fabrication of a transformer with magnetic layers. Windings have been buried in a ferrite core by using Femtosecond Laser Micromachining. Such a burying of windings avoids air gap and greatly increases primary and secondary inductances. Different technological steps from copper deposition to the realization of the grooves in the magnetic material (in the case of the buried transformer) through etching, gilding, lapping, sawing, polishing and gluing have been described. We also used a negative photoresist (SU-8) as an insulating layer and as a support for the fabrication of an air bridge to connect the center pad of the coils to the ground plane. The micro-transformer was characterized with a Vector Network Analyzer and the bandwidth was observed from 20 kHz to 7 MHz. The gain in the bandwidth is equal to 0,86. The buried conductors allow to increase the magnetizing inductance of the transformer and the shift of 45° between the primary and secondary windings allows to decrease the capacitive coupling.

Keywords: Integrated Micro-transformer, Femtosecond Laser Micromachining, Buried Windings, Ferrite

1. Introduction

1.1. Context

The significant development of embedded devices requires reduction of both weight and size for electronic components. This development is accompanied by a working frequency increase. In the field of power electronics, distributed low power supplies for specific circuits are essential nowadays. For such DC-DC converters and more precisely for switches, a close command with galvanic insulation is required. These two functionalities are usually implemented using a transformer. Design of integrated micro-transformer for low power gate driver represents an interesting challenge.

The first part of this paper is dedicated to a state-of-the-art literature review concerning integrated transformers with or without magnetic layers. The fabricated transformer

specifications and the design are given in paragraph II. The different steps to micro-fabricate the transformer are described in the third paragraph. The fourth paragraph is devoted to electrical measurements and shows proper functioning of the studied transformer. A short conclusion summarizes the content of this paper and highlights its main interests.

1.2. Interest of This Article

This study focuses on a micro-transformer with buried windings in a ferrite core. Burying is performed by using Femtosecond Laser Micromachining. This micromachining of ferrite material is the only approach that can be used for small dimensions ranging from a few tens to a few hundred of micrometers.

The use of two magnetic layers improves main characteristics of transformers such as inductance value on

the one hand, and on the other provides an electromagnetic shielding. Moreover, burying of windings avoids air gap and greatly increase primary and secondary inductances. Our approach using ferrite material is suitable for fabrication of devices operating in a wide frequency range, between some tens of kHz up to 100 MHz.

1.3. State-of-the-Art Literature Review

Integrated transformers can be classified into two types: - coreless transformers that exhibit low inductance value. They are used for high-frequency applications, usually beyond some tens of MHz. - transformers with magnetic layers that exhibit a higher inductance than coreless transformers. Running frequency range is classically less than a few tens MHz. Various magnetic material are used such as ferrite, Fe-Ni, soft magnetic alloys...

2. Coreless Transformers

Dae-Hee WEON et al. [1] have designed, fabricated, and tested 3 original helical RF transformers on high-resistivity Si substrate using stressed metal technology.

Various types of transformers such as stacked transformers, coupling stacked transformers, interleaved transformers and symmetrical transformers on GaAs substrate were studied by C. MENG et al. [2]. Inductance values range between 3 and 12nH for running frequencies up to 4GHz.

A comparative study of stack interwinding micro-transformers on silicon substrate was carried out by J. YUNAS et al. [3]. Results show that stack transformers feature high coupling as high as 0.97 but low operating frequency, less than some tens of MHz.

C. D. MEYER et al. [4] present the microfabrication and measurement of high-inductance-density, moderate-Q, air-core inductors, and transformers intended for switch-mode power supplies operating in the 100–500 MHz frequency range.

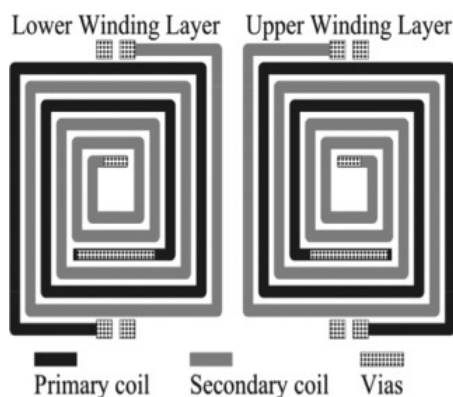


Figure 1. Air transformer structure [4].

S. Katz et al [5] propose a front-side maskless MEMS process in order to improve performances of RF-CMOS transformers and to reduce fabrication cost. The presented process is attractive for the use of transformers in system-on-chip design.

Air-core transformers are fabricated with various approaches, which are usually compatible with CMOS process. Inductance values are low and range between 1nH and a few tens of nH. The main problem concerns the low inductance/area ratio. To obtain a high inductance value one can use either a large footprint area or a magnetic material.

Ferromagnetic core transformers

A very first paper describes a new microtransformer fabricated by a dry process for use in micro-switching converters. This microtransformer is composed of CoZrRe amorphous magnetic layers wound with planar coils [6].

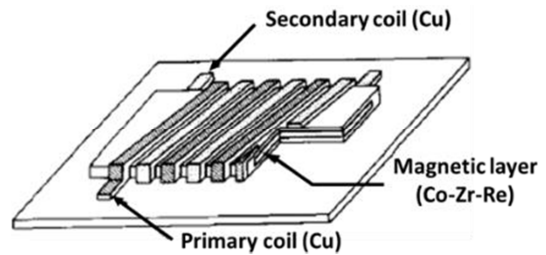


Figure 2. Transformer structure with magnetic material [6].

H. ITO [7] report the fabrication of a composite magnetic core (Fe-based amorphous/polyimide) inductor. Fe-based amorphous/polyimide composite thick film was made by screen printing consisted of 50 vol.% Fe-Si-B-Cr amorphous particles and polyimide binder.

N. WANG et al. [8] detail the design, fabrication and characterization of integrated transformers with two Ni₄₅Fe₅₅ magnetic cores. The upper and lower magnetic core are electroplated and patterned. The primary inductance reaches 210nH à 20MHz and the footprint area is equal to few mm².

Most transformers with ferromagnetic layers features high inductance and small footprint. However, they can not be used at very high frequencies due to eddy current in ferromagnetic material. Indeed, ferromagnetic materials exhibit a low resistivity. In order to operate at high frequency, it is necessary to dramatically decrease magnetic material thicknesses.

3. Ferrite Core Transformers

A Mn-Zn ferrite was used to fabricate low profile type transformers by S. ITOH et al. [9]. Two types were fabricated: one is a planar structure and the other a EI-type transformer. Inductances reach 100μH up at few hundreds of kHz.

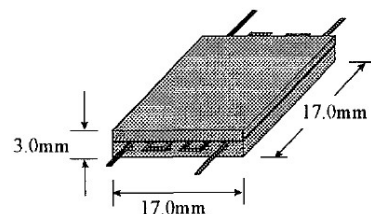


Figure 3. Transformer structure with magnetic material [9].

Micro-inductors and micro-transformers with ferrite composite magnetic core materials were fabricated and

characterized for applications up to 10MHz. [10]. The magnetic composite material was composed either of NiZn or Mn-Zn particles and polyimide.

With a similar approach, some authors have fabricated integrated power components by using screen-printing and low temperature processing technologies [11, 12].

A. MERCIER *et al* have studied and fabricated a cosintered monolithic transformers for power electronic by using Spark Plasma Sintering (SPS) [13]. The device is composed of two spiral copper coils separated by an insulating layer and encapsulated in ferrite powder.

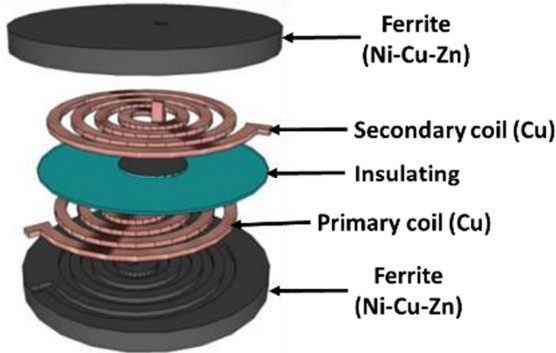


Figure 4. Fabricated Monolithic Transformer [13].

The low conductivity of this mixed-ferrite allows operation in the frequency range of 1 to 20 MHz.

An integrated interleaved transformer with two ferrite layers was studied and micro-fabricated by using microelectronics technology [14]. A proper functioning of the component was observed in the frequency range of 36MHz to 120MHz with 1.4 dB of insertion losses at 70MHz.

Most ferrite transformers are intended to be used in power electronics, particularly in DC-DC converters. For applications at low frequency less than 1MHz Mn-Zn ferrite are used. For higher frequencies, up to 100MHz, Ni-Zn ferrite, ferrite compound and specific ferrites such as YIG are used.

4. Design

The fabricated transformer is intended to be used in a driver for power switches. It has to ensure a galvanic insulation and to transfer command signals. Specifications are the following ones:

1. a primary inductance greater than 10 μ H with a small footprint area.
2. a secondary resistance of a few Ohms.
3. a low capacitive coupling: inter-windings capacitance of a few pF.
4. a frequency range up to 10MHz.

Such specifications lead to choose a transformer with magnetic core. The chosen magnetic material is the ferrite YIG (Yttrium Iron Garnet) because we are used to work with this ferrite but other ferrite like NiZn can be used. Among the main structures of winding such as stacked [15], 3D [16], interleaved [17] and Face to Face [10] the last one has been chosen. This Face to Face structure, shown Figure 5, is

composed of two windings separately fabricated on a ferrite substrate. Winding axes are rotated from each other by 45° in order to limit capacitive coupling.

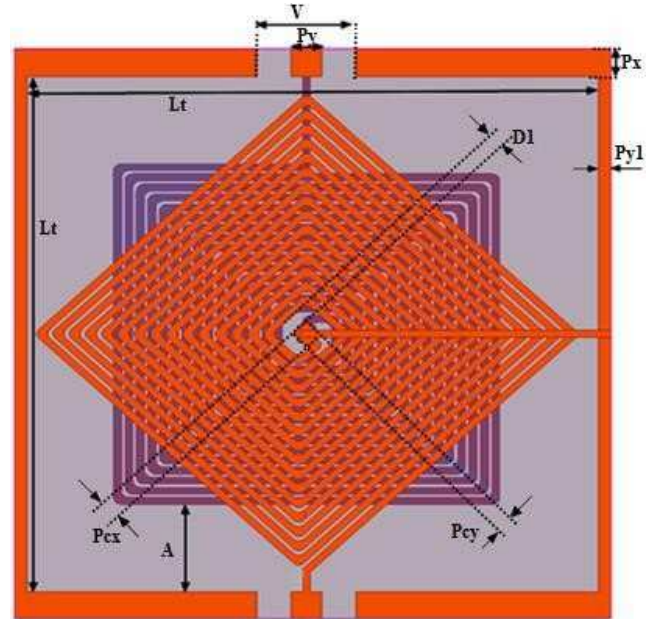


Figure 5. Top view of the device [18].

$$RDC = (\rho \times L)/S \quad (1)$$

were used for the preliminary sizing:

The RDC value leads to define the conductor cross-section

$$S = Eco * W \quad (2)$$

with Eco the conductor thickness and W the copper ribbon width.

The resistances of the primary and secondary windings of the transformer vary as function of frequency. These variations take into account proximity and skin effects with the increasing frequency [19].

The modified Wheeler's formula gives the inductance value for an air-core inductor [20]. For inductor with magnetic material the inductance is multiplied by a certain factor X , which depends on the air gap and the magnetic permeability μ_r . In our case μ_r ranges between 40 and 50, then X factor ranges between 5 and 20.

In order to obtain a high inductance value, the air-gap between primary and secondary windings has to be reduced as much as possible. In Face to Face structure air gap is equal to $Eco + Eco + Eins$. For large conductor thickness, air-gap becomes too important and decreases the inductance value. In these conditions, it is necessary to bury conductors into the magnetic material.

Using HFSS, simulations were carried out to define more accurately each parameter. HFSS software provides S_{ij} scattering parameters. Then, both impedance and admittance matrix are calculated and by means of an equivalent circuit model, electrical parameters are identified.

For example, Figure 6 shows magnetizing inductance L_F and inter-windings capacitance versus insulator thickness.

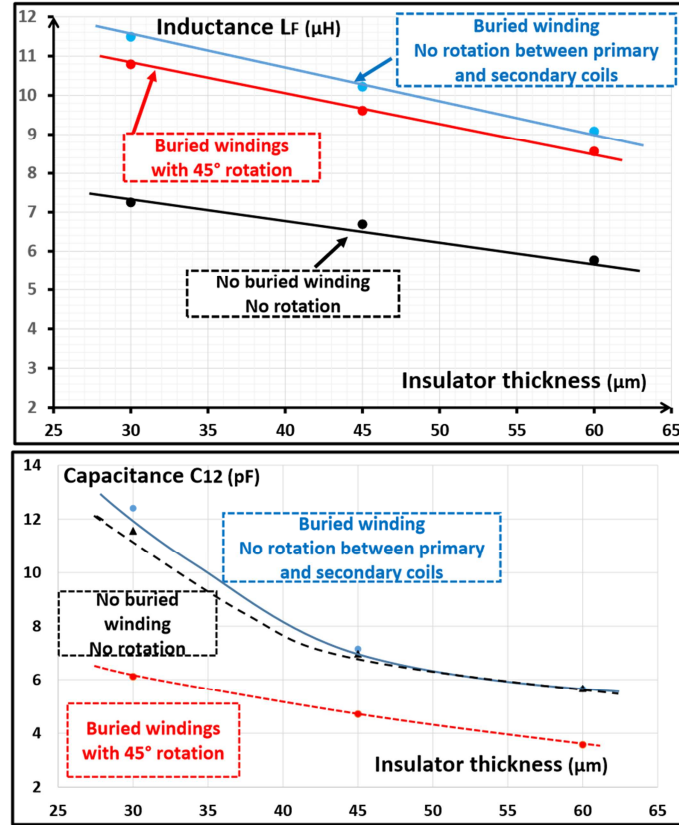


Figure 6. Magnetizing inductance according to the insulator thickness for the transformer with magnetic material in the winding.

Finally, the following parameters in table 1 were selected.

Table 1. Transformer parameters μm .

N	Winding turn	15
W	Copper ribbon width	100 μm
D	Distance between turns	60 μm
D1	Distance between the central pad and the first turn	400 μm
A	Distance between the outside turn and the ground plane	1600 μm
V	Distance between ground plane	800 μm
Px=Py	Length and width of the outside pad	500 μm
Pcx=Pcy	Length and width of the central pad	300 μm
Py1	Width of the ground plane	200 μm
LT	Device length $L=2*(A+D1+(N-1)*D+N*W)$	9430 μm
Eco	Conductor thickness	30 μm
Einsu	Dielectric thickness	30 – 95 μm
EYIG1=	Magnetic material thickness	300 – 1000

5. Fabrication

5.1. Introduction

The fabricated transformer shown Figure 7 is an integrated one with a magnetic core. It consists of magnetic, conductor and insulator stacked layers. It is made up of two almost identical half-transformers (primary and secondary) which are separately fabricated. Each half-transformer includes: - a mechanical substrate, which can be eliminated at the end of the fabrication process.

1. a ferrite magnetic layer (YIG). Its thickness can be chosen between several tens and hundreds micrometers.

2. a copper coil.
3. an air-bridge to connect the central pad to the external terminal.

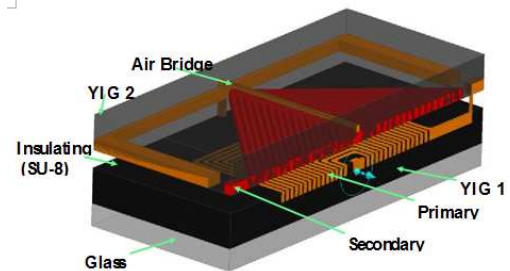


Figure 7. Transformer Face to Face.

The main fabrication steps are described hereafter.

5.2. Magnetic Layer Preparation

This first step provides a magnetic layer with appropriated sizes and a good surface finish, essential for photolithography process.

Commercial ferrite is first glued on a mechanical substrate and then cut to obtain required sizes. The next step is to grind the ferrite material to get the desired thickness. Finally, a polishing is performed to obtain a surface roughness less than 200nm.



Figure 8. Magnetic layer preparation.

5.3. Micro-machining

Windings have to be buried in the ferrite core in order to decrease air-gap and increase inductance value. Classically conductor ribbon width and depth range respectively between 400 μ m-100 μ m and 50 μ m-10 μ m. Mechanical milling is not possible for machining so small grooves. A Femtosecond laser micro-machining was used to remove material and to perform the spiral housing.

Before machining, laser beam parameters must be optimized. Laser beam diameter must be large enough to ablate a sufficient volume of material and to decrease machining time. A too large laser beam does not produce accurate dimensions for grooves. The distance between two successive pulses must be adjusted in order to restrict bottom groove roughness.

The lens focal length was chosen equal to 100mm to obtain a laser beam spot diameter of 15 μ m. A distance of 5 μ m between two successive pulses was selected.

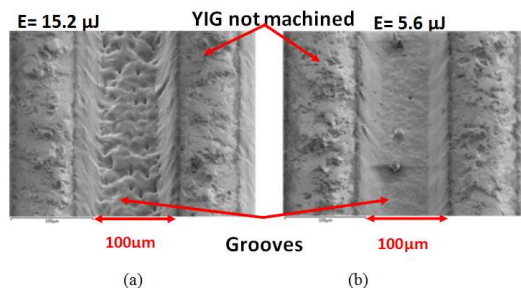


Figure 9. Influence of pulse energy on roughness, $f=150\text{kHz}$.

The machining time also depends on both repetition rate and pulse energy of laser beam. A high repetition rate and high pulse energy produce short machining time but can deteriorate the material quality in groove bottom. Indeed, a too high speed increase the ablated material temperature and can melt the material. In these conditions the material in the groove bottom can be modified and lose its magnetic features. Therefore, a 15 μ J pulse energy and repetition rate of 170kHz were selected.

Figure 9 shows two grooves obtained with two different pulse energies. By using a too strong energy pulse (Figure 9a), one can observe a great material roughness in the groove bottom.

At lower energy the machining quality is better (Figure 9b).

As an example, Figure 10 shows a micro-machined ferrite substrate with 4 coils. Each coil exhibits 6 turns and a ground plane around the coil.

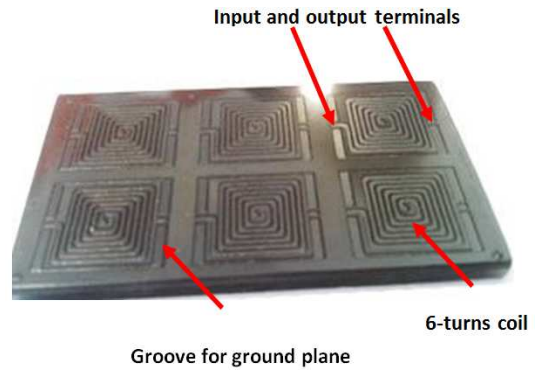


Figure 10. Example of micro-machined ferrite substrate.

5.4. Copper Coil Making

The making process of the copper coil concerns several techniques which allows:

1. a deposition of a copper layer on the micro-machined ferrite;
2. a mechanical planarization in order to eliminate copper outside grooves;
3. a surface passivation of the copper layer.

5.4.1. Copper deposition

Before deposition, substrate is properly clean. Copper layer is obtained by sputtering deposition. For the prepared devices, the layer thickness is greater than 30 μ m in order to completely fill the grooves. About 2 hours are required to achieve this process. Figure 11 shows a micro-machined ferrite substrate with a copper layer above.

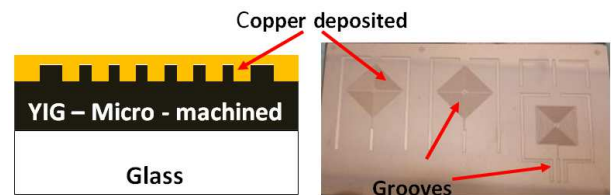


Figure 11. Insulation layer and access opening.

5.4.2. Planarization

A photolithography process and a wet etching method using iron perchlorate hydrate is classically used in our laboratory. In this case this approach is not suitable due to the large thickness of the copper layer. Because chemical etching is isotropic an important part of copper could be removed in each direction. An alternative approach was used. A mechanical polishing/planarization using polishing paste and polishing spray with 3 μ m diamond grain was performed. Figure 12 shows the planarization result.

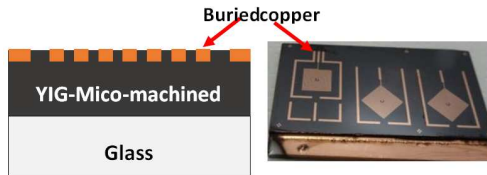


Figure 12. Device after planarization.

With atmospheric oxygen, copper reacts and forms a layer of oxide. In order to prevent oxidation, copper layer must be passivated. A thin gold layer was deposited on the copper.

5.5. Interconnection

Various solutions, such as wire bonding, flip-chip, air-bridge, can be used for connection to connect the inner pad in the center of the spiral coil to the external pad. In the case of Face to Face structure, the best solution is an air-bridge. This airbridge has to connect the inner pad in the center of the spiral coil to the external pad without any contact with the spiral coil. In order to simplify measurement, the external pad is the ground plane. The main steps are described below.

5.5.1. Insulation Layer and Access Holes

A SU-8 insulating photoresist layer is spin-coated and then patterned using a mask in order to provide access holes to copper areas. The SU8 layer thickness is slightly less than $10\mu\text{m}$. Figure 13 shows these areas: ground plane and the central pad.

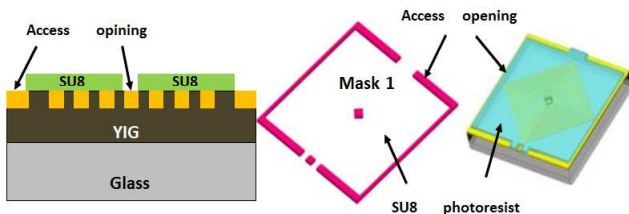


Figure 13. Insulation layer and access opening.

The insulator photoresist layer must be densified before the next copper deposition. A 30mn post-bake at 150°C is performed.

5.5.2. Filling Access Holes

The access holes have to be filled before the last step related to air-bridge making. Thus, a copper layer is deposited by sputtering in order to fill access holes. About 40mn are required to achieve this copper deposition. Figure 14 illustrates this step, copper is deposited in access holes as well as on the SU8 photoresist.

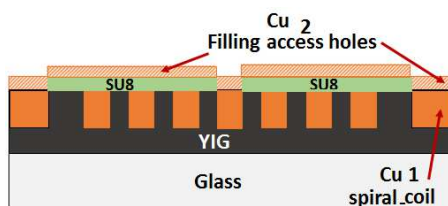


Figure 14. Filling access hole.

The copper layer deposited on the SU8 photoresist must be removed. A photolithography process and a wet etching method was used to removed less than $10\mu\text{m}$ of copper. The positive photoresist SPR 505 and an iron perchlorate solution were used. Figure 15 shows a sectional view at the end of this step.

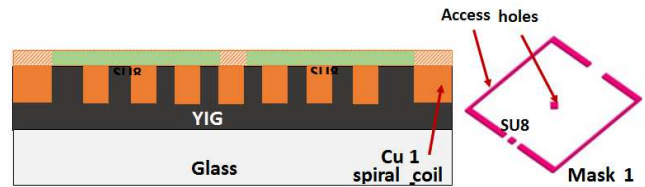


Figure 15. Photolithography process and wet etching.

5.5.3. Air-Bridge Making

Classical processes were performed for this last step. First of all, a copper layer was deposited by sputtering. The copper layer thickness is about $5\mu\text{m}$. Afterwards, the photolithography process was performed using SPR 505 photoresist, followed by a wet etching.

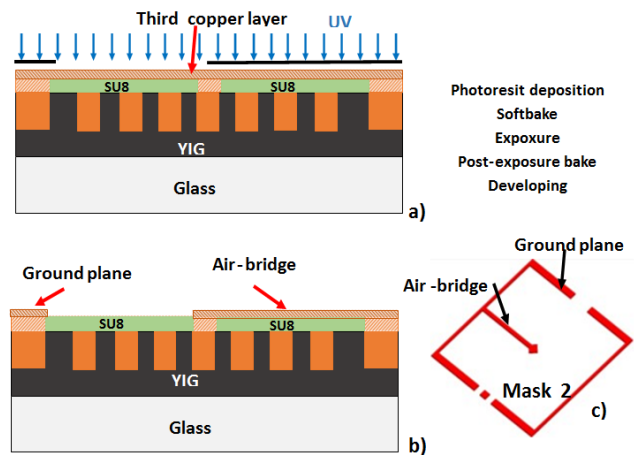


Figure 16. Making process of the air-bridge.

Figure 16b shows the sectional view of the final device, which corresponds to a half part, primary or secondary, of the Face to Face transformer. To avoid oxidation, both ground plane and air-bridge are passivated by using a gold electrodeposition process. Figure 17 shows the final two half part devices.

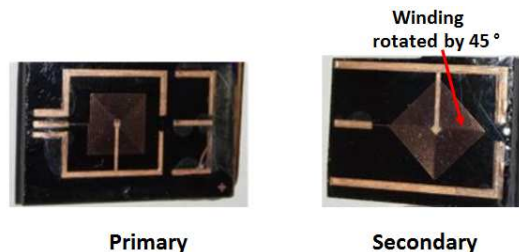


Figure 17. Making process of the air-bridge.

5.6 Transformer Assembly

The two parts, i.e. primary and secondary windings, were

glued together. An electrically conductive ink was used to assemble the two parts of the transformer. The electrical conductive ink contains silver particles and exhibits an excellent electrical conductivity. Due to the low thickness of the deposited silver glue and its high conductivity, the contact resistance is negligible compared to coil one. Figure 18 shows the fabricated transformer.

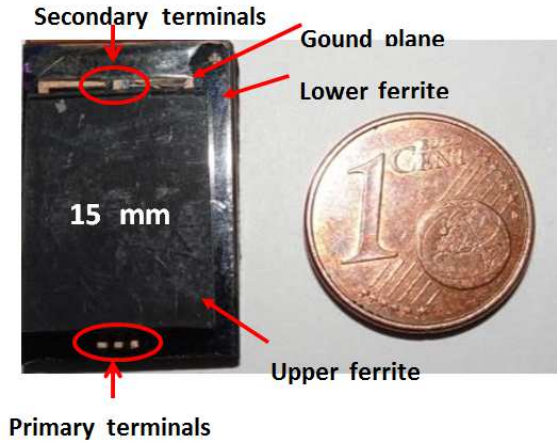


Figure 18. Transformer Face to Face.

5.7. Electrical Characterization

To verify the proper operation of the transformer, its frequency response was determined [20]. A sinusoidal signal was applied to the primary winding and the secondary voltage was measured. First of all, we made sure that the secondary wave remains sinusoidal. Then, a measure of magnitude and phase of the output as a function of frequency, in comparison to the input was performed, as shown Figure 19.

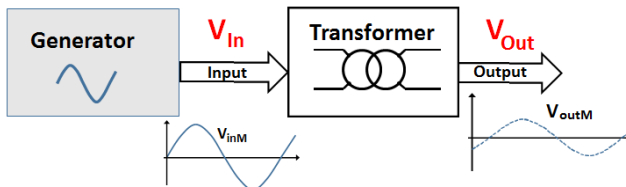


Figure 19. Principle of the electrical measurement.

Figure 20 shows the frequency response of the transformer in open circuit conditions. Gain versus frequency is only plotted.

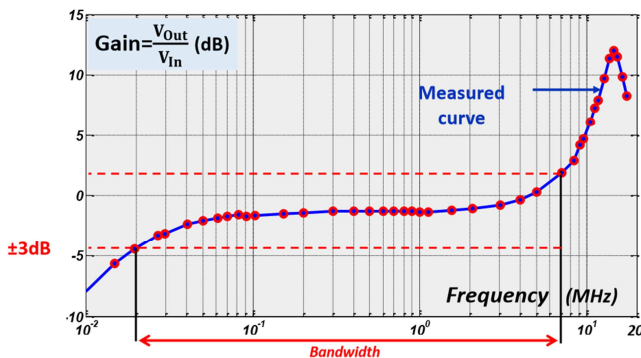


Figure 20. Transformer frequency response.

One can observe a 3dB bandwidth which ranges between 20kHz and 7MHz. The gain in the bandwidth is equal to 0,86. A resonance due to stray capacitance occurs at 15MHz.

6. Conclusion

The main steps of the micro-fabrication of a transformer with magnetic layers and buried windings has been presented. To bury windings in the ferrite core a Femtosecond Laser Micromachining has been used. Such a burying of windings avoids air gap and greatly increase primary and secondary inductances. Measurements have been carried out to show the electrical performance of the fabricated device.

This work could also be extended to the study of power transformers (in the Watt range) and to the realization of isolated DC-DC micro-converters. For these "high" powers, the thermal aspects cannot be neglected and must be deeply studied.

References

- [1] D.-H. Weon and Saeed Mohammadi. (2007). High-Inductance-Density, AirCore, Power Inductors, and Transformers Designed for Operation at 100–500 MHz. *IEEE High Performance 3-D Helical RF Transformers*, pp. 1897-1900. Doi: 10.1109/TMAG.2010.2045742.
- [2] Chinchun Meng, Ya-Hui Teng, Yi-Chen Lin, Jhin-Ci Jong and YingChieh Yen. (2007). Characteristics of Integrated RF Transformers on GaAs Substrates. *IEEE Proceeding of Asia-Pacific Microwave Conference*, pp. 1.4. Doi: 10.1109/APMC.2007.4554720.
- [3] Jumril Yunas, Burhanuddin Yeop Majlis. (2008). Comparative study of stack interwinding micro-transformers on silicon monolithic. *Microelectronics Journal*, vol. 39, issue. 12, pp. 1564-1567. Doi: 10.1016/j.mejo.2008.02.026.
- [4] Christopher D. Meyer, Sarah S. Bedair, Brian C. Morgan, and David P. Arnold. (2010). High-Inductance-Density, Air-Core, Power Inductors, and Transformers Designed for Operation at 100–500 MHz. *IEEE Transactions On Magnetics*, vol. 46, pp. 2236-2239, Juin 2010. DOI: 10.1109/TMAG.2010.2045742.
- [5] Shlomo Katz, IgorBrouk, SaraStolyarov, ShyeShapira, YaelNemirovsky. (2012). High performance MEMS 0.18 μm RF-CMOS transformers. *Microelectronics Journal*, vol. 43, pp. 13-16. DOI: 10.1109/COMCAS.2009.5386016.
- [6] Masato Mino, Toshiaki Yachi, Akio Tago, Keiichi Yanagisawa, and Kazuhiko Sakakibara. (1992). A New Planar Micro-transformer for Use in Micro- Switching Converters. *IEEE Transactions On Magnetics*, vol. 28, pp. 1769-1773, Juillet-Août 1992. DOI: 10.1109/20.144755.
- [7] Hideyuki Ito, Asako Takeuchi, Shinya Okazaki, Hiroki Kobayashi, Yuichiro Sugawa, Akihiro Takeshima, Makoto Sonehara, Nobuhiro Matsushita and Toshiro Sato. (2011). Fabrication of Planar Power Inductor for Embedded Passives in LSI Package for Hundreds Megahertz Switching DC-DC Buck Converter. *IEEE Transactions On Magnetics*, vol. 47, pp. 3204-3207. DOI: 10.1109/TMAG.2011.2147288.

- [8] Ningning Wang, Santosh Kulkarni, Brice Jamieson, James Rohan, Declan Casey, Saibal Roy, Cian O'Mathuna. (2012) High Efficiency Si Integrated MicroTransformers Using Stacked Copper Windings for Power Conversion Applications. *IEEE Enterprise Ireland UTIM*, pp. 411-416. Doi: 10.1109/APEC.2012.6165852.
- [9] Satoru Itoh, Yutaka Yamamoto, Akihiro Makino, Takashi Yamaguchi, Ichiro Sasada. (1998). A low Profile Type High Frequency Transformer Using a fine Grained Mn-Zn Ferrite. *IEEE Power Electronics Specialists Conference*, pp. 1492-1498. DOI: 10.1109/PESC.1998.703261.
- [10] J. Y. Park, L. K. Lagorce, M. G. Allen. (1997). Ferrite Based Integrated Planar Inductors and Transformers Fabricated at Low Temperature. *IEEE Transactions On Magnetism*, vol. 33, N°5, September 97. DOI: 10.1109/20.617931.
- [11] Dong H. Bang and Jae Y. Park. (2009). Ni-Zn Ferrite Screen Printed Power Inductors for Compact DC-DC Power Converter Applications. *IEEE Transactions On Magnetism*. vol. 45, pp. 2762-2765. Doi: 10.1109/TMAG.2009.2020550.
- [12] K. I. Arshak, A. Ajina, D. Egan. (2001). Development of screen-printed polymer thick film planar transformer using Mn-Zn ferrite as core material. *Microelectronics Journal*, vol. 32, pp. 113-116. DOI: 10.1016/S0026-2692(00)00122-1.
- [13] A. Mercier, K. Zehani, G. Chaplier, A. Pasko, V. Loyau and F. Mazaleyrat. (2015) SPS co-sintered monolithic transformers for power electronic. *IEEE Transaction on Magnetism*, vol. 4, pp. 1-4. Doi: 10.1109/TMAG.2015.2504876.
- [14] Faouzi KAHLOUCHE, Youssef KHAMIS, Mahamat hasan BECHIR, Stephane CAPRARO, Ali SIBLINI, Jean Pierre CHATELON, Cyril BUTTAY, Jean Jacques ROUSSEAU. (2014). Fabrication and characterization of a planar interleaved micro-transformer with magnetic core. *Microelectronics Journal*, vol. 45, pp. 893-897. <https://doi.org/10.1016/j.mejo.2014.03.003>
- [15] Alireza Zolfaghari, Andrew Chan, and Behzad Razavi. (2000). Stacked Inductors and 1 to 2 Transformers in CMOS Technology. *IEEE Custom Integrated Circuits Conference*, pp. 620-628. Doi: 10.1109/CICC.2000.852681.
- [16] Lei Gu and Xinxin Li. (2007). High-Performance CMOS-Compatible Solenoidal Transformers With a Concave-Suspended Configuration. *IEEE Transaction on microwave theory and Techniques*, vol. 55, pp. 1237-1245. Doi: 10.1109/TMTT.2007.897853.
- [17] Fu Jian, Mei Niansong, Huang Yumei, and Hong Zhiliang. (2011). CMOS high linearity PA driver with an on-chip transformer for W-CDMA application. *Journal of Semiconductors*, vol. 32, pp. 1-6. DOI: 10.1088/1674-4926/32/9/095006.
- [18] T. Mahamat, B. Danoumbé, M. Youssouf, J. P. Chatelon, S. Capraro, and J.J. Rousseau, (2016). Optimization of integrated magnetic planar transformer. *IEEE Proc. Eur. Conf. Power Electron. Appl. (EPE)*, p 1-8, Sep. 2016. DOI: 10.1109/EPE.2016.7695386.
- [19] A. Abderahim, O.B. Arafat, A. Ouzer Nabil, Y. Dagal Dari. (2021). Windings losses of planar components determination from current density. *International Journal of Engineering Sciences & Research Technology*. Vol. 10, No. 11, November 2021, pp. 46 – 53. <http://www.ijesrt.com/November-2021.html>
- [20] Sunderarajan S. Mohan, Maria del Mar Hershenson, Stephen P. Boyd, and Thomas H. Lee. (1999). Simple Accurate Expressions for Planar Spiral Inductances. *IEEE Journal of Solid-State Circuits*, Vol. 34, NO. 10, october 1999, pp 1419-1424. DOI: 10.1109/4.792620.
- [21] D. A. Oumar, M. I. Boukhari, M. A. Taha, S. Capraro, D. Piétroy, J. P. Chatelon, J. J. Rousseau. (2019). Characterization Method for Integrated Magnetic Devices at Lower Frequencies (up to 110 MHz). *Journal of Electronic Testing: Theory and Applications (JETTA)*. <https://doi.org/10.1007/s10836-019-05790-3>. pp. 245 – 251.